How to measure the resilience of a fully renewable multi-vector energy system?

Gabriela Vera-Hofmann[1], Simón Moreno-Leiva[2], Felipe Díaz-Alvarado[1], Ludger Eltrop[3], and Jannik Haas[2]

[1]University of Chile, Santiago (Chile)

[2]Department of Stochastic Simulation and Safety Research for Hydrosystems (IWS/SC SimTech), Stuttgart (Germany)

[3]Institute of Economics and Rational Energy Use (IER), Stuttgart (Germany)

Abstract

The ability of a system to endure and recover after extreme events, its resilience, is an aspect of its performance that is often neglected. There are abundant studies on the analysis of the resilience of systems in the fields of transportation and infrastructure. Its application in the design of energy systems is rather scarce and bounded to electric power systems. Considering the ongoing multisectoral transition toward renewable energy systems, we foresee the need for a resilience index that is suitable to be integrated into multi-vector energy system planning. For the sake of computational tractability, most optimization models for energy system planning aim at linearity. The goal of this work is to propose a resilience index that is suitable for multi-energy systems planning and that allows the modelers to maintain the linearity of the optimization problems. First, we review the existing literature on resilience indicators and further analyzed those that we considered could be adapted for our objectives. Then, we propose an indicator and provide an example of its application for the ex-post analysis of the resilience of a case-study system. Finally, we test the system under different scenarios for the recovery time and the level of damage in the components. The resulting resilience indicator behaves consistently among the scenarios and we expect that it will be easy to integrate it as an optimization goal in models for multi-energy system planning. Integrating this kind of indexes at the early stages of the planning process would allow modelers to conceive more robust energy systems for the future.

Keywords: Resilience, optimization, multi-energy systems, natural disasters, multi-objective planning

1. Introduction

The need to mitigate climate change has fostered the use of renewable energies (Sawin, Rutovitz, and Sverrisson 2018). For reaching high shares of renewables, coupling different energy sectors using multi-energy (heat, power, fuels) systems has proven beneficial in smoothing out the variability of renewable sources (e.g. photovoltaics PV) (Brown et al. 2018; Mancarella 2014). Multi-energy systems (MES) consider different energy vectors -like electricity, heat, and fuels- and coordinate the operation of the infrastructure to reach, for example, minimum costs. MES can improve economic and environmental performance as compared to classical configurations, where the supply of different forms of energy or services are treated separately (Mancarella 2014). MES, like any other system, are vulnerable to damage in extreme events, such as earthquakes, which may result in a disruption of the energy supply (FEMA 2015).

The ability to recover from damage is called resilience. This term is widely used in multiple disciplines, including psychology, ecology, environment, among others. However, the shared use of resilience implies the ability of an entity or system to return to normal conditions after the occurrence of an event that disrupts its state (Hosseini, Barker, and Ramirez-Marquez 2016). To graphically represent resilience, the *resilience curve* is used. This curve represents the system's health over time (Panteli and Mancarella 2015), as shown in Fig. 1. In the beginning, the system is in a steady state with health Q_0. In time t_0, an event occurs, which causes a reduction of the system's health, reaching the value Q_e. After the event, the system starts a recovery state, until it reaches again the former steady state in time t_{rec}.

doi:10.18086/swc.2019.31.06 Available at http://proceedings.ises.org

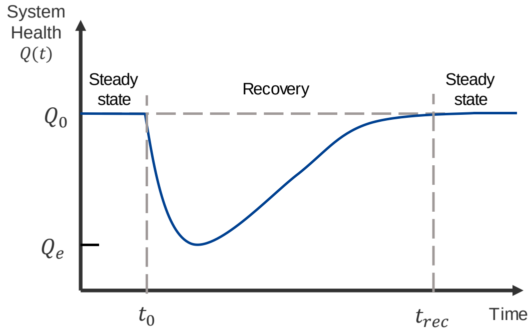

Fig. 1: Graphic representation of a resilience curve.

Some authors studied different ways to measure resilience, proposing metrics for different application areas (Bruneau et al. 2003; Zobel 2010). Literature reveals that there is no unique way to describe the concept, however, they agree on the ability to recover. Despite the recent works on resilience, resilience metrics for power systems have not been completely studied. In particular, a resilience indicator for coupled multi-energy systems has not been observed. This study aims at filling this gap.

The goal of this work is, first, to provide a review of the academic literature on available resilience metrics. Secondly, based on this review, we will propose a new resilience indicator for multi-energy systems that can be used in the optimal planning of energy systems. The novelty of this study is the index definition and its area of application. It is aimed at being used in the design phase of MES, in linear programming optimization models.

Section 2 shows a literature review of resilience metrics. Section 3 explains the proposed indicator and Section 4 illustrates its ex-post application on a case study. Section **¡Error! No se encuentra el origen de la referencia.** discusses the case study and the limitations of the indicator. Finally, Section 5 draws the conclusions.

2. Review: Resilience indexes

This section reviews the existing literature on resilience indexes. We revise 60 studies on resilience, then we select those that we considered that can be adapted to energy system planning and analyzed them in more detail. First, we show the field of application of the articles, then we offer more details on the selected ones.

Resilience is applied to many engineering fields. In Fig. 2, we summarize the application area of the reviewed studies. The most studied field is infrastructure and transportation, while resilience in power systems accounts for a minor share. Although there are some studies that use resilience metrics in power systems, a resilience indicator for multi-energy systems has not been observed. Accordingly, the indicator we introduce in the next sections aims at filling this gap.

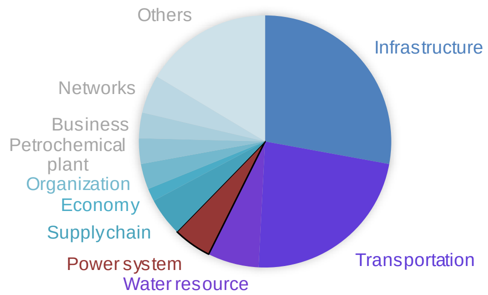

Fig. 2: Application area of the different metrics. 60 metrics analyzed.

From the revised studies on resilience, we select some metrics that we consider can be adapted to the field of MES. The selected metrics are summarized in Tab. 1. The metrics are described with some specific features: type of extreme event, the application area, uncertainty considerations (deterministic or probabilistic), and time modeling (dynamic or stationary). In the following, we summarize the selected studies.

Tab. 1 Some resilience metrics proposed in literature

Reference	**Resilience Metric**	**Recover from**	**Application area**	**Deterministic/ probabilistic**	**Stationary/ dynamic**
(Bruneau et al. 2003)	$R = \int_{t_0}^{t_1} [100 - Q(t)]dt$	Earthquakes	Infrastructure	Deterministic	Dynamic
(Bruneau and Reinhorn 2007)	$R = \int_{t_0}^{t_1} [100 - Q(t)]dt, \quad Q(t) = 100 - [L \cdot f_{rec} \cdot \alpha_R]$	Earthquakes	Infrastructure	Probabilistic	Dynamic
(Zobel 2010)	$R(X,T) = 1 - \frac{XT}{2T^*}$	-	-	Deterministic	Dynamic
(Zobel 2011)	$R(X,T) = 1 - \frac{XT}{2T^*} + \alpha\left(\frac{XT}{2T^*}\right)$	-	-	Deterministic	Dynamic
(Afgan and Veziroglu 2012)	$R_j = \sum_i w_i \int_{t_0}^{t_1} [100 - q_i(t)]dt$	-	Power systems	Deterministic	Dynamic
(Enjalbert et al. 2011)	$R_L = \frac{dS(t)}{dt}, \quad R_T = \int_{t_b}^{t_e} \frac{dS(t)}{dt}$	Human accident occurrences	Transportation	Deterministic	Dynamic
(Chen and Miller-Hooks 2011)	$R = E\left(\sum_w d_w / \sum_w D_w\right)$	Natural or human caused disaster	Transportation	Deterministic	Dynamic
(Franchin and Cavalieri 2015)	$R = \frac{1}{P_d E_0} \int_0^{P_d} E(P_r)dP_r$	Earthquakes	Infrastructure	Probabilistic	Dynamic
(Rose 2007)	$R = \frac{\%DDY^m - \%DDY}{\%DDY^m} = \frac{Y_D - Y_0}{Y_N - Y_0} = \frac{B}{A}$	-	Economy	Deterministic	Stationary
(Omer, Nilchiani, and Mostashari 2009a)	$R_{network} = \frac{V_{init} - V_{loss}}{V_{init}}$	Undersea earthquakes, fish bites or ship anchors	Networks	Deterministic	Stationary
(Henry and Ramirez-Marquez 2012)	$R = \frac{Recovery(t)}{Loss(t_d)} = \frac{F(t_r \mid e_j) - F(t_d \mid e_j)}{F(t_0) - F(t_d \mid e_j)}$	External disruptive event	Transportation	Deterministic	Stationary
(Baroud et al. 2014)	$R_\varphi(t_r \mid e^j) = \frac{\varphi(t_r \mid e_j) - \varphi(t_d \mid e_j)}{\varphi(t_0) - \varphi(t_d \mid e_j)}$	-	Water resource	Probabilistic	Stationary
(Barker and Ramirez-marquez 2016)	$R_\varphi(E,[0,T_C]) = \frac{\frac{1}{\lvert E \rvert}\sum_E \int_0^{T_C} \varphi(t;N,L,C)}{\int_0^{T_C} \varphi^{nominal}(t;N,L,C)}$	Terrorist attacks, natural disasters or manmade hazards	Infrastructure	Probabilistic	Dynamic

Bruneau et al. (2003) propose an indicator to measure the size of the expected degradation in quality (Q) over time due to an earthquake. This metric is deterministic and dynamic. Later, Bruneau and Reinhorn (2007) improved the same index with a more detailed measure of functionality. It considers the loss function (L), which is measured as the ratio of the actual loss, the recovery function (f_{rec}) after the time occurrence, which depends on the resources available during the recovery period, and the functionality recovery factor (α_R). The second term considers probability fuctions from fragility curves (Masanobu Shinozuka et al. 2000), being a probabilistic index.

Zobel (2010) proposed a simplification of the metric proposed by Bruneau et al. (2003). They calculated the loss function as a linear function and the total loss of functionality as the area of a triangle, in terms of the initial impact (X) and the recovery time (T). They also incorporated a time horizon (T^*), which allows to represent resilience as a percentage (Zobel 2010). Later, Zobel (2011) adjusted this resilience function by giving different importance (α) to the initial impact of the disaster event and to the recovery time, by adding a new parameter to adjust the slope of the resilience function.

The metric proposed by Afgan and Veziroglu (2012) was also based on Bruneau et al. (2003) index. However, they developed a resilience index considering sustainability dimensions, which is a linear agglomeration function of products between indicators and the corresponding weighting coefficients (w_i).

Enjalbert et al. (2011) defined the concept of *local resilience* (R_L) and *total resilience* (R_T), where the local resilience is an instantaneous measurement of resilience and is the slope of the resilience curve (S). It can be negative or positive if the performance decreases or increases, respectively. The total resilience is the sum of local resilience during a given period.

Chen and Miller-Hooks (2011) developed a similar indicator to that of Zobel (2010), measuring the fraction between the loss and total functionality. In this case, they define resilience as a fraction between the demand that can be satisfied after the event (d_w) and the pre-disaster satisfied demand (D_w).

Franchin and Cavalieri (2015) described resilience in a new field: civil infrastructure. Their metric is a measure of the reallocated population ($E(P_r)$) due to an earthquake. They also considered uncertainty and vulnerability factors and how they affect resilience.

All the above-mentioned metrics consider the behavior of the system over time to measure resilience. There are other stationary indexes (Baroud et al. 2014; Henry and Ramirez-Marquez 2012; Omer, Nilchiani, and Mostashari 2009b; Rose 2007), which measure the robustness of the system. These indexes are defined as a fraction between the system health after the event and before. They just differ in their application field.

3. A new indicator

In this section, and based on the literature review, we propose a new metric to measure the resilience of a multi-energy system. First, we describe a multi-energy system with a generic superstructure. Later, we explain mathematically the newly proposed indicator.

MES are systems where different energy vectors interact with each other. They consider different types of technology (as shown in Fig. 3): primary generation PG, transformation technologies TT (from one type of energy to another), storage S of the different energy types, and the process D which demands energy. Examples of energy vectors are: heat, fuels, and electricity. There can be several technologies for the generation of one type of energy (e.g. photovoltaics PV and wind turbines for electricity generation). For the transformation technologies, in the generic model, every transformation is possible (e.g. heat to fuel, electricity to heat, etc.). Depending on the application, some of them might not be considered.

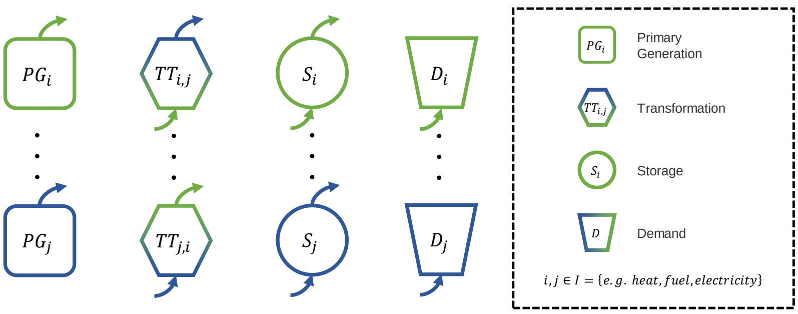

Fig. 3: Model superstructure.

The proposed indicator considers the possible shortage of energy in the system due to an earthquake. This indicator requires as inputs the performance of the energy technologies (energy demand and supply over time, considering efficiency and generation profile for variable renewable energy), the energy demand, and the technologies behavior in the case of facing an earthquake, which includes the damage state and the reposition time (how long it takes for this technology to recover and be available again (FEMA 2015)).

The indicator we propose describes the resilience of the system as a percentage that shows the energy that the system can supply after a disruptive event about the total energy demand in an evaluation horizon. To determine the energy that the system can supply, we need to measure the non-supplied energy (energy shortage) of each energy vector to obtain the total shortage. This is analog to the loss of energy expectation (LOEE) in power systems but extended to multi-vector systems using weighting factors and considering models for the recovery of the components after an extreme event. We evaluate the damage of each component of the system and count the energy demand that cannot be satisfied as a result of this damage. This is done for each vector and the total resilience is a weighted sum.

As this indicator quantifies the possible energy shortage to the process, we need to know the behavior of each technology during the time, represented in their power capacity. This is illustrated in Fig. 4, where the maximum power available is described by $P^{av}(t)$. This power can be mathematically described as follow:

$$P^{av}(t) = \begin{cases} P^{inst} & , \quad t < t_0 \\ P^{inst} \cdot (1 - \mathbb{E}(x)) + mt & , \quad t_0 \leq t < t_{rec} \\ P^{inst} & , \quad t \geq t_{rec} \end{cases} \qquad \text{(eq. 1)}$$

Where P^{inst} is the power of one technology previously installed, $\mathbb{E}(x)$ is the expected failure value (share of the capacity that is not operative), t_0 is the time of the day where the event occurs, t_{rec} the expected recovery time, and T^* the time period of the evaluation.

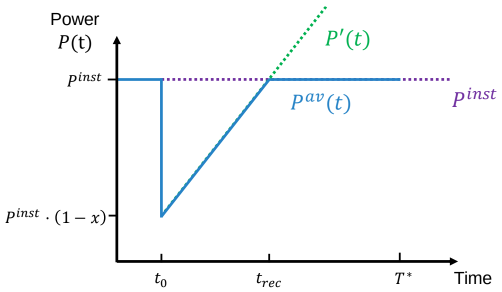

Fig. 4: Power vs. Time

The energy delivered or consumed by each technology changes over time. Fig. 5 a) shows in orange line a possible power delivered $P(t)$ from a technology, i.e. the power which was scheduled to deliver. But it got damage and now can deliver maximum $P^{av}(t)$ (blue line). Hence, the resulting operation of this technology after an event is $P_r(t)$ (purple line), as it shows Fig. 5 b).

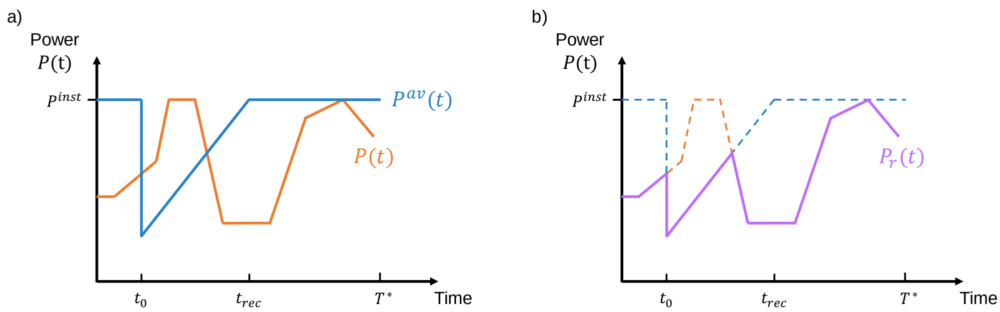

Fig. 5: Power delivered or consumed by each technology due to an event.

Mathematically, this is expressed as the minimum between both functions:

$$P_r(t) = \min\{P^{av}(t),\ P(t)\} \qquad \text{(eq. 2)}$$

And in LP, the constraints are the following:

$$P_r(t) \leq P^{av}(t) \qquad \text{(eq. 3a)}$$

$P_r(t) \leq P(t)$ $\qquad$ $P_r(t) \leq P^{av}(t)$ (eq. 3b)

We do the same procedure for each technology.

To define the resilience of the system, we need to measure the non-supplied energy. Therefore, we measure the energy shortage (Sh) in every time for each energy type $\left(ShP_i(t)\right)$, through an energy balance. This balance is the difference between the demand and the supply of that energy type. The energy demand is the sum of the demand of the process P_D^i, the demand of the transformation technologies $P_{TT}^{i,j}$, which demand i to produce j and the energy required by the storage load $P_S^{load,i}$. The supply corresponds to the energy produced from the primary generation P_{PG}^i, the supply from the transformation technologies $P_{TT}^{j,i}$, and the energy given by the storage unload $P_S^{load,i}$. This can be summarized in the next equation:

$$ShP_i(t) = \left(P_D^i + \sum_j P_{TT}^{i,j} + P_S^{load,i}\right) - \left(P_{PG}^i + \sum_j P_{TT}^{j,i} + P_S^{unload,i}\right) \qquad \text{(eq. 4)}$$

If this difference is positive means that there is an energy shortage if it is negative means that the system can supply the demand. So, the shortage is the maximum between this difference and zero:

$$ShP_i^+(t) = \max\left(0, ShP_i(t)\right) \qquad \text{(eq. 5)}$$

And in LP, the constraints are the following:

$$P_r(t) \leq P^{av}(t) \qquad \text{(eq. 6a)}$$

$P_r(t) \leq P(t)$ $\qquad$ $P_r(t) \leq P^{av}(t)$ (eq. 6a)

The total energy shortage is summed over time:

$$Sh_i = \int_{t_0}^{T^*} ShP_i^+(t)\,\mathrm{dt} \qquad \text{(eq. 7)}$$

With this shortage, we can calculate the resilience for this energy vector as one minus the fraction between the energy shortage and the demand of that vector:

$$R_i = 1 - \frac{Sh_i}{E_D^i} \qquad \text{(eq. 8)}$$

As it is a multi-vector energy system, the total resilience is the sum of the weighing of all resilience:

$$R_T = \sum_i \left(R_i \cdot \frac{E_D^i}{\sum_i E_D^i}\right) = \frac{\sum_i E_D^i - \sum_i Sh_i}{\sum_i E_D^i} \qquad \text{(eq. 9)}$$

4. Application of the resilience indicator

In this section, we study the application of the proposed index. We use a study case of a fully renewable multi-energy system and we discuss the obtained results. Then we study the behavior of the indicator on different scenarios for damage and recovery time.

The topology of the study case is presented in Fig. 6. This is a simplification of a previously reported system (Moreno et al. 2018). It consists of a fully renewable multi-energy system that supplies the energy demand for a copper mine, which demands energy in the form of electricity, heat, and hydrogen. Specifically, our case of study considers PV for the primary generation of electricity, lithium batteries for electricity storage, and hydrogen storage. In the transformation technologies, we consider a heating rod to produce heat from electricity and an electrolyzer to produce hydrogen using electricity.

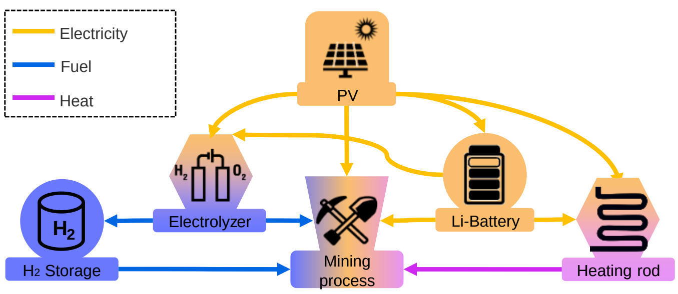

Fig. 6: Structure of the system for the case study.

This system is planned with two targets: minimizing cost and minimizing the global warming potential of the installation and operation (Moreno et al. 2018). We will measure the resilience of this system with the proposed indicator. This exercise measures the resilience of the system *as it is*, without considering the possibility of adapting the operation or oversizing components in the design. In other words, this is an ex-post analysis where the resilience index has not been integrated into the optimization model for the system's design.

To study the application of the indicator we use an evaluation time (T^*) of 3 months and the process-demand is shown in Tab. 2. For the damage and the recovery time of each technology we assigned values (as it is shown in

Tab. 3) and later we do a multi-scenario analysis to study the behavior of the indicator with different inputs for the fraction of damage and the recovery time.

The values were obtained by adapting the data from HAZUS method (FEMA 2015) for a PGA (peak ground acceleration, a measure of the intensity of an earthquake) of 0.6g (similar to the earthquake in Chile in 2010). We used the expected values for the damage state and recovery time (see Tab. 3). As the recovery function is linear in our model, these parameters completely define the function.

Tab. 2: Demand of each energy vector and total demand in a time horizon of 3 months. Values in (GWh). Obtained from (Moreno et al. 2018)

Electricity Demand	874
Heat Demand	40
Fuel Demand	46
Total Demand	960

Tab. 3: Damage fraction and recovery time of each technology (FEMA 2015).

	PV	**Electrolyzer**	**Heating Rod**	**Li-Battery**	**H_2 Storage**
Damage fraction	0.91	0.79	0.85	0.79	0.81
Recovery time (h)	5472	2255	10141	2255	2313

Tab. 4 shows the resulting resilience value for each energy vector and the total system resilience.

Tab. 4: Resilience of each energy vector and total resilience.

Electricity Resilience	63%
Heat Resilience	27%
Fuel Resilience	64%
Total Resilience	62%

We can see that the resilience for the heat vector has the lowest value. This is because there is only one technology to provide heat and it has a long recovery time. This low value does not have a big impact on the total resilience because the heat demand in the case study is low. The energy vector that has the highest weight on the total resilience is electricity because it has the highest demand.

The value of resilience also depends on the time horizon (which is an arbitrary decision) and the PGA of the earthquake. A value of 62% of resilience for this case, means that for a PGA of 0.6, this system can provide the 62% of the total energy demand in three months. This is equivalent to a blackout that lasts one month, which we consider would be a long period of time.

To study the behavior of the indicator with different inputs for the damage state and recovery time, we do a scenario analysis. We vary the values of these parameters by ±20% and study the resulting total resilience in each case. The results are shown in Tab. 5.

Tab. 5: Total resilience of the system for different scenarios for the deviation from the original parameters.

		Deviation of the damage		
		-20%	**0**	**+20%**
Deviation of the Recovery time	**-20%**	79%	66%	58%
	0	77%	62%	52%
	+20%	75%	59%	48%

We can observe, as it is expected, that the highest resilience value is reached with the lowest damage and recovery time, reaching 79%. Conversely, the minimum resilience value is obtained when the damage and the recovery time increase. Tab. 6 shows the percentual change on resilience for every scenario, as compared to the original resilience.

We can see that the highest growth, when both parameters decreased, is 29%, but when we increase both parameters in the same percentage, the resilience decrease by 22%. Also, we can notice that changing the damage state causes a higher percentual change than varying the recovery time. For example, increasing the damage by 20% decreased resilience by 15%, while increasing the recovery time in the same percentage, resilience decreased just by 5%.

Tab. 6: Comparison of the total resilience values in Tab. 5 as a deviation from the original resilience value.

		Damage		
		-20%	**0**	**+20%**
Recovery time	**-20%**	+29%	+7%	-6%
	0	+24%	0%	-15%
	+20%	+21%	-5%	-22%

The system in the case study depends fully on solar PV for primary energy generation, so it is important to consider the weather. In the present analysis, the time of the earthquake t_0 was fixed in the first hour of the year (00:00, January 1). Since the case study is in Chile (southern hemisphere), that is in the summertime. Then, the availability of solar energy is higher than at other times of the year. To compensate for the reduced capacity factor in winter, the system has more installed capacity of PV than it requires in summer. This would lessen the impact of losing generation capacity during this season. In other words, it should be harder for the system to compensate the same damage in solar generation during winter than during summer. Analyzing the effect of the timing of disruptive events on the resiliency of highly solar multi-energy systems is an interesting topic for further research, which could be tackled using the proposed indicator.

As

There

Also,

The

In contrast to other resilience metrics, this indicator can be easily integrated into the planning process. This is because of the linear nature of the index. Using LP is common practice in energy systems planning. This allows for computational tractability in large scale problems. Including our index allows modelers to keep the optimization linear. It can be included, for example, as an optimization goal. However, to use it in planning decisions, it needs some minor adaptation. For example $Prt \leq P^{av}(t)$ (eq. 3a) is no longer needed, as the power delivered should be just less than the power available and the installed capacity. $P_r(t) \leq P(t)$

5. Conclusions

The resilience metrics that are available in the scientific literature differ in the event the system recovers from, the application area, if it considers uncertainty or not, and if it considers the time and dynamics of the system. The literature review has shown a lack in the study of resilience metrics for power systems, specifically, there is no study observed for multi-energy systems. Accordingly, we propose a resilience indicator for multi-energy systems that can be easily integrated into linear optimization models for energy system planning. Some hurdles are identified in the implementation of this kind of resilience index. Specifically, in the consideration different forms of uncertainty, the definition of the temporal scope, and the weighting criteria.

To study the application of the developed indicator, we use a case study and to study the indicator behavior, we do a scenario analysis, changing the damage and reposition time in ±20%. The damage state causes the highest variation in the system resilience (around ±20%), while varying the reposition time causes a variation form around ±6%.

The proposed indicator can be integrated into the planning process, using it, for example as a target in an optimization. Therefore, in the future, we expect to integrate this indicator in real case planning, through a multi-objective optimization, considering two targets: costs and resilience. This allows us to give different importance to each target and analyze the trade-off of planning with resilience.

Acknowledgments

This work was supported by the German Academic Exchange Service (DAAD) and the Chilean National Commission of Technology and Science [grant number CONICYT PFCHA/DOCTORADO BECAS CHILE BILATERAL DAAD/2016 – 62160012; CONICYT/FONDAP/15110019; CONICYT/FONDECYT/1181532], and the German Research Foundation [grant number DFG-NO 805/11-1].

References

Afgan, Naim and Ayfer Veziroglu. 2012. "Sustainable Resilience of Hydrogen Energy System." *International Journal of Hydrogen Energy* 37(7):5461–67.
Barker, Kash and Jose E. Ramirez-marquez. 2016. "Infrastructure Network Resilience." *IRGC Resource Guide on Resilience* 1–7.
Baroud, Hiba, Jose E. Ramirez-Marquez, Kash Barker, and Claudio M. Rocco. 2014. "Stochastic Measures of Network Resilience: Applications to Waterway Commodity Flows." *Risk Analysis* 34(7):1317–35.
Brown, T., D. Schlachtberger, A. Kies, S. Schramm, and M. Greiner. 2018. "Synergies of Sector Coupling and Transmission Reinforcement in a Cost-Optimised, Highly Renewable European Energy System." *Energy* 160:720–39.
Bruneau, Michel, Stephanie E. Chang, Ronald T. Eguchi, George C. Lee, Thomas D. O'Rourke, Andrei M. Reinhorn, Masanobu Shinozuka, Kathleen Tierney, William A. Wallace, and Detlof Von Winterfeldt. 2003. "A Framework to Quantitatively Assess and Enhance the Seismic Resilience of Communities." *Earthquake Spectra* 19(4):733–52.
Bruneau, Michel and Andrei Reinhorn. 2007. "Exploring the Concept of Seismic Resilience for Acute Care Facilities." *Earthquake Spectra* 23(1):41–62.
Chen, Lichun and Elise Miller-Hooks. 2011. "Resilience: An Indicator of Recovery Capability in Intermodal Freight Transport." *Transportation Science* 46(1):109–23.
Enjalbert, Simon, Frédéric Vanderhaegen, Marianne Pichon, Kiswendsida Abel Ouedraogo, and Patrick Millot. 2011. "Human Modelling in Assisted Transportation." *Human Modelling in Assisted Transportation* 335–41.
FEMA. 2015. *Hazus –MH 2.1*. Washington, D.C.
Franchin, Paolo and Francesco Cavalieri. 2015. "Probabilistic Assessment of Civil Infrastructure Resilience to Earthquakes." *Computer-Aided Civil and Infrastructure Engineering* 30(7):583–600.
Henry, Devanandham and Jose Emmanuel Ramirez-Marquez. 2012. "Generic Metrics and Quantitative Approaches for System Resilience as a Function of Time." *Reliability Engineering and System Safety* 99:114–22.
Hosseini, Seyedmohsen, Kash Barker, and Jose E. Ramirez-Marquez. 2016. "A Review of Definitions and Measures of System Resilience." *Reliability Engineering and System Safety* 145:47–61.
Mancarella, Pierluigi. 2014. "MES (Multi-Energy Systems): An Overview of Concepts and Evaluation Models." *Energy* 65:1–17.
Masanobu Shinozuka, By, Honorary Member, Maria Q. Feng, Associate Member, Ho-Kyung Kim, and Sang-Hoon Kim. 2000. *NONLINEAR STATIC PROCEDURE FOR FRAGILITY CURVE DEVELOPMENT*.
Moreno, Simon, Jannik Haas, Tobias Junne, and Ludger Eltrop. 2018. "A Green Copper Concept: On the Design of a Full-Renewable Energy Supply for Its Production." in *International Symposium on Energy System Optimization*. Karlsruhe.
Omer, Mayada, Roshanak Nilchiani, and Ali Mostashari. 2009a. "Measuring the Resilience of the Global Internet Infrastructure System." *2009 IEEE International Systems Conference Proceedings* (November):156–62.
Omer, Mayada, Roshanak Nilchiani, and Ali Mostashari. 2009b. "Measuring the Resilience of the Global Internet Infrastructure System." Pp. 156–62 in *2009 3rd Annual IEEE Systems Conference*. IEEE.
Panteli, M. and P. Mancarella. 2015. "The Grid: Stronger, Bigger, Smarter?" *IEEE Power & Energy Magazine* 13(3):58–66.
Rose, Adam. 2007. "Economic Resilience to Natural and Man-Made Disasters: Multidisciplinary Origins and Contextual Dimensions." *Environmental Hazards* 7(4):383–98.
Sawin, J., J. Rutovitz, and F. Sverrisson. 2018. *Renewables 2018-Global Status Report*. Paris.
Zobel, Christopher W. 2010. "Comparative Visualization of Predicted Disaster Resilience." *The 7th International Conference on Information Systems for Crisis Response and Management (ISCRAM)* (May):1–6.
Zobel, Christopher W. 2011. "Representing Perceived Tradeoffs in Defining Disaster Resilience." *Decision Support Systems* 50(2):394–403.